ICEMG 2020-XXXXX

Effects of the Rotor Slot Dimensions on Performance Characteristics of the 3-phase Squirrel Cage Induction Motors

Mahdi Rezaiee Nakhaie[1], **Reza Roshanfekr**[2]

[1] Master of Science student, Hakim Sabzevari University, Sabzevar; rmehdi356@gmail.com
[2] Assistant Professor, Hakim Sabzevari University, Roshanfekr@hsu.ac.ir

Abstract
There are different approaches to improve the performance characteristics of induction motors, however, the approaches with deals to the rotor slot shape have important effects on performance characteristics. In this paper, two approaches include a new design of the rotor slot based on the rotor slot of the conventional model, and also the changing of the rotor slot shape is employed to improve the performance characteristics of the 30-kW, 3-phase, 4-poles, 48-stator slots, and 44-rotor squirrel cage induction motor. Comparison of analytical, simulation and experimental results confirm the proposed FEM-based model of 30-kW induction motor. Based on this model, the sensitivity analysis of efficiency, starting torque, and power factor considering the variations of the rotor slot dimensions have been accomplished. Furthermore, the genetic algorithm (GA) is considered to redesign of the rotor slots to improve the efficiency. The results of the GA-based optimal design of the rotor slot dimensions showed a 0.32% improvement in motor efficiency. On the other hand, the starting torque is increased by 37.93% and also the power factor has a 0.55% reduction in comparison with the conventional model.

Keywords: Induction motor, Squirrel cage, Efficiency, Starting torque, Power factor, Optimization, Genetic Algorithm

I. Introduction

Squirrel cage induction motors are extensively used in many industrial fields due to their simple structure, reliability, low cost, less maintenance and ability to work in inimical environments. Since the starting torque in an induction motor is poor, there is a limitation to be used in some applications requiring high starting torque. One of the ways to increase the starting torque is changing the resistance and reactance of the rotor, especially the top part of rotor slot resistance due to the skin effect in the motor startup. The slot depth design is another procedure to improve the starting torque, however, this design increases rotor slot leakage reactance and decreases motor efficiency. Besides, the efficiency of these motors should pay particular attention due to the wide applications in industry. According to the results of an investigation for the US Federal Energy Administration**,** the electric motors consume 64% of the total electric consumption in the United-state. Thus, energy conservation requires focusing on electric motors, and their efficiencies [1]- [3].

As the rotor bar shape has more important effects on motor performance characteristics, there are many studies about rotor bar design. In some studies, the rotor slot shape has been changed to increase starting torque, efficiency or achieve a certain torque-speed curve, [1]-[5]. In the other studies, changing the slot dimensions and rotor slot area is employed to improve the motor performance characteristics [6]- [8].

Furthermore, the aluminum die-cast process of the rotor bars and end rings, the porosity phenomena occur in bars and end rings of the rotor. As the porosity is proportional to the fill factor reversely, the results show that the efficiency and starting torque will be increased by 1.92 %, and 11.93 %, whereas the fill factor is changed from 62% to 93%, respectively [9], [10]. But, in the industry, the fill factor is usually over 96 % and also it is difficult to model in software design.

The skewed rotor bars are employed to reduce the harmonic components of motor specifications. For instance, the total harmonic distortion (THD) of stator current with the skewed model is reduced by 44.1% in comparison with the without skewed model [11]. Also, the novel skewed rotor presented in [12], decreases the radial electromagnetic force as well as the noise of the motor. Furthermore, the inclination of rotor bars which is different from the skewing of rotor bars, increased both the efficiency and starting torque is increased by 0.63 % when the inclination angle adjusted from 0^{o} to 25^{o}, respectively [13]. However, the rotor bar inclination is limited when the number of rotor slots increases.

The main goal of this paper is changing the rotor slot dimensions and the shape of the rotor slot to improve the motor efficiency, however, the effects of this variation are investigated on the power factor and starting torque too. This paper is written in the following way. The motor performance characteristics have been determined based on the mathematical equations related to the magnetic equivalent circuit and the geometric dimensions of the induction motors. Then, the motor performance characteristics obtained from mathematical equations have been compared with the simulation results and experimental tests. Also, two approaches with a combination of the genetic algorithm have been applied to the conventional model to improve motor efficiency, starting torque, and power factor. Finally, according to the comparison of the results, the optimal approach is chosen.

II. Analytical Equations

The performance characteristics of the induction

motors can be determined according to their geometric dimensions, and rated parameters. In this section, the mathematical equations related to the motor efficiency, power factor, and starting torque are described which they are proportional to the magnetic equivalent circuit parameters of the motor [14]. The parameters of the magnetic equivalent circuit which include stator resistance (R_s), rotor resistance (R_r), stator reactance (X_s), rotor reactance (X_r), and magnetization reactance (X_m), can be described as follow:

A. Magnetic Equivalent Circuit Parameters

The stator resistance can be calculated according to the Eq. (1):

$$R_s = \rho(l_c W)/(A.a) \tag{1}$$

where ρ is the copper resistivity, l_s is coil length, W is the number of turns per phase, A is the cross-sectional area of the coil, and a is the number of parallel branches.

The rotor resistance reduced to the stator can be described as follow:

$$R_r = (4mW^2.K_w^2.R_{be})/N_r \tag{2}$$

where m is the number of phases, N_r is the number of rotor slot, K_w is the stator winding coefficient, and R_{be} is the resistance of the bar and end-ring segments.

The reactance is proportional to the shape of the slot. So, it will be different for different slots. In general, the rated stator reactance can be expressed by Eq. (3):

$$X_s = 2\mu_0.\omega.L(2W^2/p.q)(\lambda_s + \lambda_{ds} + \lambda_{ec}) \tag{3}$$

where μ_0 is the vacuum permeability, ω is the angular velocity, L is the stack length, q is the number of stator slot per pole, p is the pole pairs, and λ_s, λ_{ds}, and λ_{ec} are the slot conductivity, differential, and end connection conductivity coefficient respectively.

The reactance of the rotor reduced on the stator is calculated according to the Eq. (4):

$$X_r = (4mW^2.K_w^2.X_{be})/N_r \tag{4}$$

where X_{be} is the reactance of the bar and end ring segments equivalent which can be calculated as follow:

$$X_{be} = 2\pi f\ \mu_0 L(K_x\lambda_r + \lambda_{dr} + \lambda_{er}) \tag{5}$$

where f is the frequency, K_x is the skin effect coefficient for the leakage reactance, and λ_r, λ_{dr}, and λ_{er} are the slot conductivity, differential, and end ring conductivity coefficient respectively.

In general, the ratio of the rotor resistance to rotor bar/end-rings segments equivalent resistance in rated speed equals the ratio of the rotor resistance to rotor bar/end-ring segments equivalent resistance at zero speed. Thus, the rotor resistance in rated speed can be calculated as follow:

$$R_r^{rated} = \left(R_r^{zero}.R_{be}^{rated}\right)/R_{be}^{zero} \tag{6}$$

The reactance of the rotor in the rated speed is calculated in a similar way.

B. Efficiency

As the Efficiency (η) is proportional to the total losses, it can be expressed using Eq. (7):

$$\eta = P_{out}/(P_{out} + P_{loss}) \tag{7}$$

where, P_{out} is the rated output power, and P_{loss} is the total power losses of the motor. The total motor losses can be divided into iron loss, stator copper loss, rotor copper loss, mechanical loss, and stray loss. So:

$$P_{loss} = P_{iron} + P_s + P_r + P_m + P_{stray} \tag{8}$$

where P_m is the mechanical loss, P_{stary} is the stray loss. and

$$P_s = 3R_s I_n^2 \tag{9}$$

$$P_r = 3R_r K_I^2 I_n^2 \tag{10}$$

where R_s is the stator resistance, R_r is the rated rotor resistance, I_n is the rated current, and K_I is the coefficient of the stiffness stator MMF relative to the rotor.

The core loss P_{iron} consists of the fundamental P^l_{iron} and harmonic P^h_{iron} iron loss. The fundamental iron loss occurs only in the stator teeth (P^l_t) and stator yoke (P^l_y) due to the rotor frequency is low. The stator teeth fundamental loss P^l_t and the stator yoke fundamental loss P^l_y can be calculated approximately using Eq. (11) and (12):

$$P_t^1 \approx K_t \times P_1 \times (f_1/50)^{1.3} B_{ts}^{1.7} G_{ts} \tag{11}$$

$$P_y^1 \approx K_t \times P_1 \times (f_1/50)^{1.3} B_{ys}^{1.7} G_{ys} \tag{12}$$

where P_1 is specific losses in W/Kg at 1.0 Tesla and 50Hz, K_t is coefficient core loss augmentation due to the mechanical machining, f_1 is the fundamental frequency, G_{ts} is stator tooth weight, G_{ys} is stator yoke weight, B_{ts} is tooth flux density, and B_{ys} is yoke flux density.

The power factor can be expressed using Eq. (13):

$$\cos\varphi = P_{out}/3V_{ph}I_n\eta \tag{13}$$

where V_{ph} is phase voltage.

C. Torque

In general, the induction motor torque can be expressed using Eq. (14):

$$T = \frac{3V_{ph}^2 \times (R_r/S)}{\omega([R_s + (R_r/S)]^2 + [X_s + X_r]^2)} \tag{14}$$

where S is the slip.

The starting torque T_s based on the starting current I_{start} is calculated according to the Eq. (15)

$$T_s = (3R_r^{zero} I_{start}^2/\omega)p \tag{15}$$

III. Conventional Model

In this paper, the three design approaches are applied on a 3-phase squirrel cage induction motor which identified in Table 1, and also the cross-section of the stator and rotor core, slot shape of stator and rotor of this motor are showed in Figure 1.

According to the theoretical equations (Section II) and the motor geometrical dimensions, the performance characteristics of the conventional model have been calculated. Also, this model has been simulated by Maxwell software which operates based on the finite element method (FEM).

Table 1. **Specifications of the 3-phase squirrel cage induction motor as the conventional model**

Specifications	Value
Rated Output Power (kW)	30
Number of Poles	4
Rated Speed (rpm)	1474
Rated Voltage (V)	380
Rated Current (A)	57.2
Stator Outer radius (mm)	163.5
Rotor Outer radius (mm)	104.35
Stator Opening Slot (mm)	3.8
Rotor Opening Slot (mm)	1.5
Depth of the Stator Slot (mm)	26.8
Depth of the Rotor Slot (mm)	38
Degree of the Rotor Slots Skewing	3.48

Table 2. **The induction motor performance characteristics obtained from theoretical analysis, experimental test, and simulation results**

Characteristics	Theoretical	Experimental	Simulation
I_n (A)	54.23	57.359	53.62
I_{start} (A)	230.21	226.65	234.22
PF (%)	92.0	87.1	90.0
P_{iron} (W)	1244	965	454.92
P_s (W)	742.8	909	770.77
P_r (W)	335.6	564	315.66
P_{loss} (kW)	2.8	2.95	2.1
η (%)	91.14	91.518	93.59
T_s (N.m)	330.36	482.4	339.82

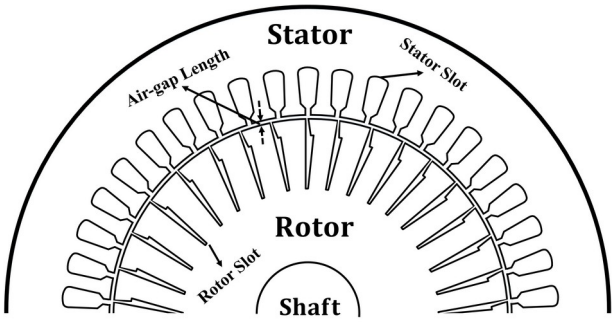

Figure 1. Cross-section of the stator and rotor core related to the conventional model

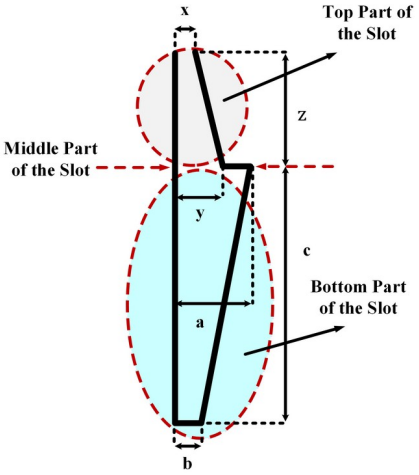

Figure. 2 Rotor slot shape of the conventional induction motor

In order to that, the conventional motor is a commercially motor which is used in industry, the experimental tests of this motor are available. The results of the theoretical analysis, experimental test, and simulation of the conventional model have been presented in Table 2. In this table, PF is the power factor, P_{loss} is the total losses.

The determined performance characteristics given in Table 2, are relatively close to each other, except η and P_{iron}. Based on the opinion of the professional engineers in the field of electric motor manufacturing, the iron loss is augmented due to the mechanical machining which is considered as a coefficient (K_t) in Eq. (11) and (12) to calculate the iron loss. So, the efficiency obtained from simulation can be modified considering the K_t coefficient.

IV. Sensitivity Analysis

Since the induction motor is influenced by the skin effect at motor startup conditions, the current is concentrated in the top part of the rotor slot whereas the current flows of the whole slot at the motor rated conditions. Therefore, various parts of the rotor slot and their shape have effects on the performance characteristics of the motor. Hence the effects of changing the rotor slot dimensions along both width and depth are investigated on the motor efficiency, power factor and starting torque. Furthermore, when the dimensions of the rotor slot are changed, the total rotor slot area, as well as the current density, losses and efficiency of the rotor slot, is no longer equal to its previous value.

The motor efficiency, power factor, and starting torque versus width and depth dimension variations of the rotor slot are illustrated in Figure 3, and 4, and 5 respectively. Based on Figure 3-a, an increase of the top part of the rotor slot width (x-dimension) makes the reduction of efficiency however as the middle part width of the rotor slot (y-dimension) becomes larger, the efficiency is increased continuously. Also, the bottom part width (b-dimension) increase results in a sharper reduction in efficiency in comparison with other parts (3.2% reduction from beginning to end of the curve).

The power factor is changed similarly to the efficiency based on Figure 4-a. Furthermore, the starting torque related to the different parts of the rotor slot width has been shown in Figure 5-a. As the current is concentrated in the top part of the rotor slot, this part has a great effect on the starting torque. Furthermore, the starting torque related to middle part width is increased however it is less than the top part width variations. Also, the bottom part width has no significant effects on starting torque as shown in Figure 5-a.

According to Figure .3-b, the top part of the rotor slot depth (z-dimension) has no significant effects on efficiency so that it is almost constant. However, increasing the bottom part depth of the slot (c-dimension) is directly related to efficiency.

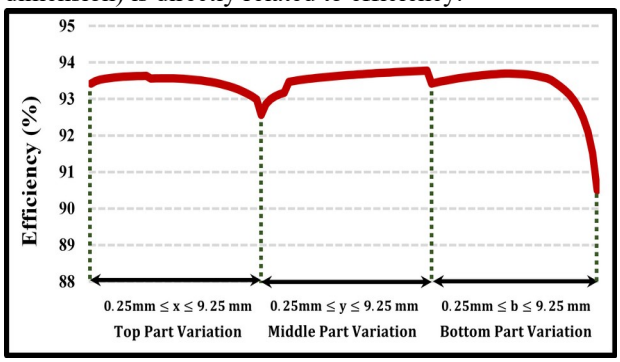

(a)

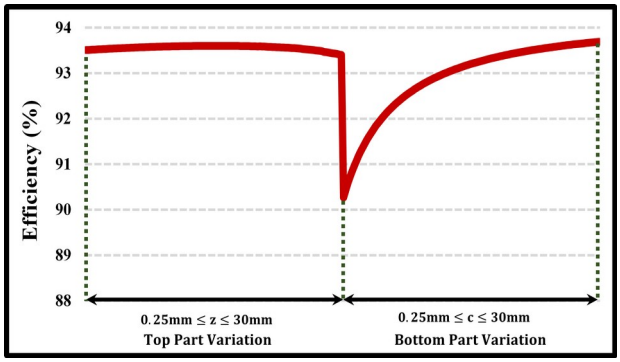

(b)

Figure 3. Different part sensitivity of the rotor slot dimensions on the efficiency of the conventional model. (a)- Width Parts, (b)- Depth Parts

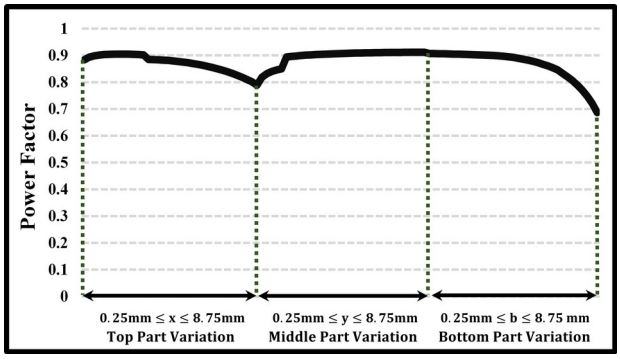

(a)

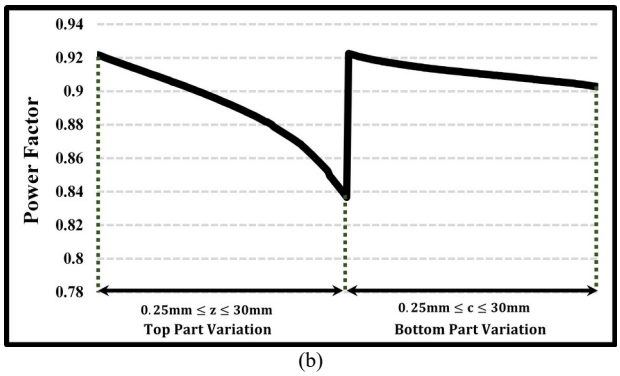

(b)

Figure 4. Different part sensitivity of the rotor slot dimensions on performance characteristics of the conventional model. (a)- Width parts, (b)- Depth parts

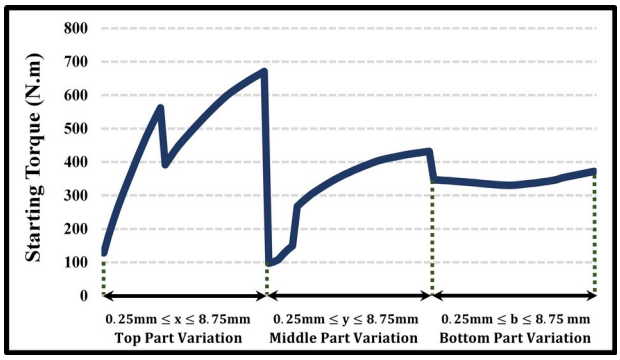

(a)

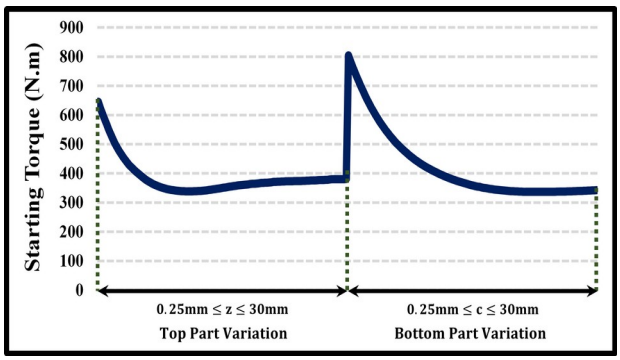

(b)

Figure 5. Different part sensitivity of the rotor slot width on performance characteristics of the conventional model. (a)- Width parts, (b)- Depth parts

If the bottom part depth is increased from 0.25mm to 40mm, the efficiency was increased by 4%. Furthermore, the power factor is treated similarly to the efficiency curve (Figure .4-b). Also, Figure .5-b shows that the slot with deep depth has a lower starting torque.

V. Motor Design Approaches

The rotor slot shape is proportional to the resistance and reactance of the rotor so that when the dimensions of the rotor slot are changed, the resistance and the reactance of the rotor slot is no longer equal to their previous value. Therefore, the rotor slot shape has great effects on the performance characteristics of the induction motors. In this paper, the rotor slot shape of the conventional model is designed with combinations of

the genetic algorithm (GA) to satisfy the highest motor efficiency. In addition, the overall shape of the rotor slot is changed with the four slot type to investigate the performance characteristics of the conventional model. Then, each slot shape is redesigned with GA to improve the motor efficiency. The results of the sensitivity analysis are used to determine the design parameter limits in the optimization process which the objective function is satisfied.

A. The Rotor Slot Design Based on the Conventional Model Slot Shape

The rotor of the conventional model offers efficiency by the amount of 93.59% which is an acceptable value. Anyway, in this approach, the rotor slot shape of the conventional model is redesigned to investigate the increase or decrease of motor efficiency. In other words, the goal is to design an optimal rotor slot based on the rotor slot shape of the conventional model which offers higher efficiency in comparison to the conventional model. Hence, the maximum motor efficiency has been chosen as the objective function. The optimization algorithm has six variables such as x, z, y, a, c, b which are the dimensions of the conventional model rotor slot (Figure .5-a). The results of the GA optimization are presented in Table 3 and also the optimal rotor slot shape using GA is depicted in Figure .5-b.

The simulated performance characteristics of the optimal motor have been presented in Table 4. The results show that the optimal slot shape offers higher efficiency so that the motor efficiency increases by 0.32% in comparison with the conventional model efficiency. Besides, this slot offers the lower power factor and the higher starting torque and starting current. The power factor is reduced by 0.55%, and the starting torque is increased by 18.13% in comparison with the starting torque of the conventional model.

B. Changing of the Rotor Slot Shape

As mentioned before, the shape of the slot is proportional to the reactance of the slot which affects motor efficiency. Hence, in this approach, the rotor slot shape has been changed to investigate the effect of different slot shapes on motor performance characteristics considering constant slot area (134.2 mm^2). The motor performance characteristics related to the conventional model and each rotor slot shapes (shown in Figure .6) are presented in Tables 5. According to the results, the highest efficiency is 93.63 % in I, III, and IV prototypes. In these cases, the efficiency increases by 0.04 % in comparison with the efficiency of the conventional model.

To optimize the presented prototypes of the rotor slot shape, the objective function considered maximum motor efficiency. Figure .7 shows the prototype and GA-based optimal shapes of the case I. In this optimal slot shape, the motor efficiency increased the amount of 0.21%, and 0.29% in comparison with the conventional model (Figure .2), and the prototype case I, respectively. Figures .8, and 9 show the prototype and GA-based optimal shapes of cases II, and III, respectively. The efficiency of the optimal model in Figure .8 increases by 0.32%, 0.28% in comparison with the conventional model, and the prototype case II, respectively. Also, the efficiency in the GA-based optimal shape of case III (Figure .9) increases by 0.31%, and 0.27% in comparison with the conventional model, and the prototype case III, respectively. The efficiency, power factor and starting torque results of all considered slot cases in this approach have been illustrated in Figure .10, 11, and 12 respectively. Based on efficiency case II has the highest efficiency between all cases. However, the power factor in both cases II, and III is reduced by 0.88% while it is an increased amount of 1.5% by case I in comparison with their prototype power factor. In addition, based on Figure .12, the starting torque by case I is almost constant (0.6% increment) but in case II, and III the starting torque is increased by 15.25%, and 4.9% in comparison with their prototype starting torque. So, based on the higher increase of efficiency, and starting toque, and also with respect to the low reduction in power factor by case II, this case is chosen as the optimal rotor slot in approach 2. As mentioned before, the sensitivity analysis of the rotor slot dimensions showed that the suitable slot shape for higher efficiency is the slot with a tight top, and bottom width, wide middle width, and deep depth. The results of the GA validate the sensitivity analysis results.

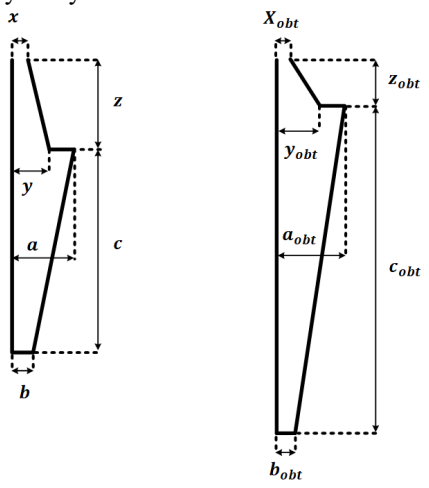

Figure 5. Rotor slot shape. (a)- Conventional model, (b)- Optimal model related to the approach 1

Table 3. The results of the genetic algorithm optimization

Variables	Limits (mm)	Initial value (mm)	Optimal value (mm)
x (mm)	0.75-2.25	1.5	1.509
z (mm)	5-15	10	5.900
y (mm)	1.75-5.25	3.5	4.605
a (mm)	2.9-8.7	5.8	7.876
c (mm)	14-42	28	38.039
b (mm)	1-3	2	1.549

Table 4. The induction motor characteristics of the optimal rotor slot shape related to approach

1 In comparison with the conventional model (simulation results)

Characteristics	Conventional	Optimal
η (%)	93.59	93.89
PF	0.904	0.899
I_{start} (A)	234.22	307.68
T_s (N.m)	339.82	401.45

Table 5. The induction motor performance characteristics related to approach 2 based on the shape in comparison with the conventional model (simulation results)

Characteristics	Conv.	I	II	III
η (%)	93.59	93.52	93.63	93.63
PF	0.904	0.876	0.912	0.912
I_{nstar} (A)	234.22	413.8	311.7	306.87
T_s (N.m)	339.82	647.66	472.74	468.72

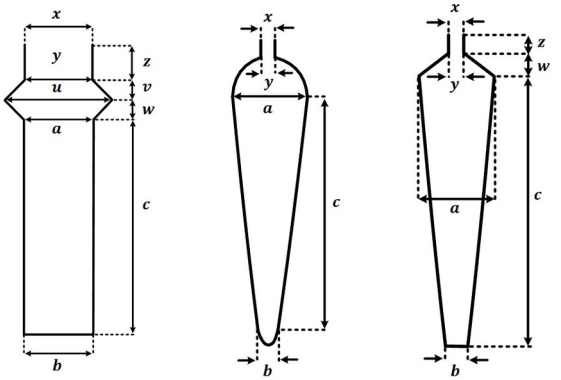

(I) (II) (III)

Figure 6. Five different prototypes of rotor slot shapes with the same area

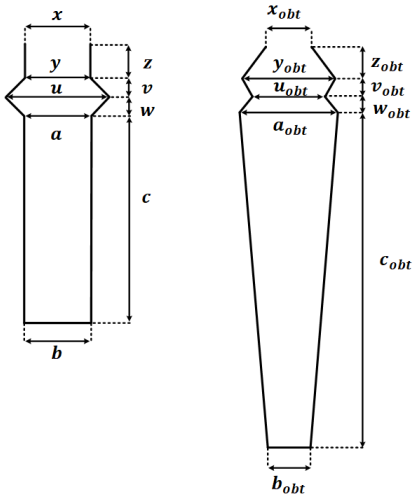

(a) (b)

Figure 7. Rotor slot shape. (a)- The prototype I, (b)- Optimal model of the prototype I

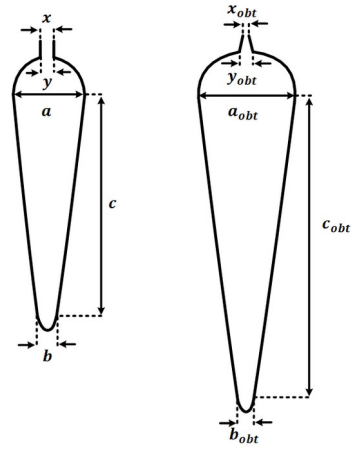

(a) (b)

Figure 8. Rotor slot shape. (a)- The prototype II, (b)- Optimal model of the prototype II

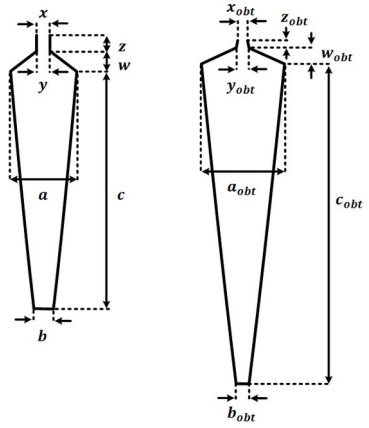

(a) (b)

Figure 9. Rotor slot shape. (a)- Prototype III, (b)- Optimal model of prototype III

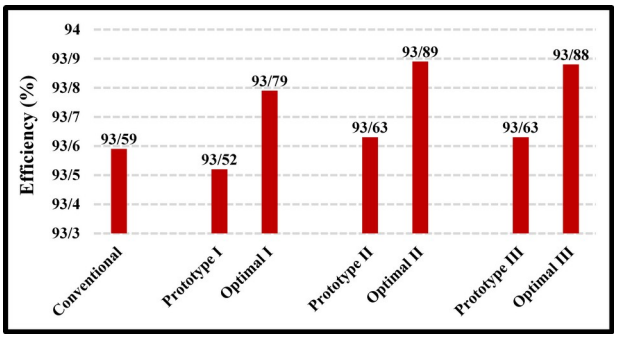

Figure 10. The efficiency of the prototype and the optimal shape of the slots related to the approach 2

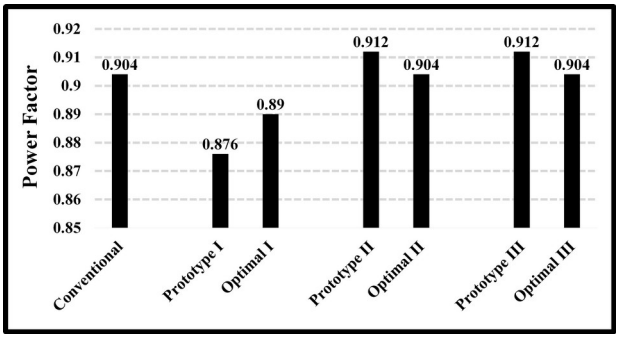

Figure 11. The power factor of the prototype and the optimal shape of the slots related to the approach 2

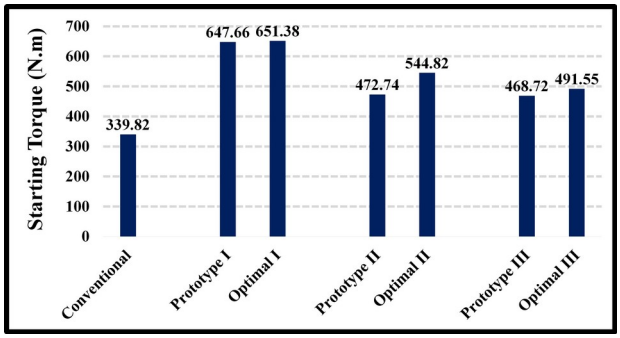

Figure 12. The starting torque of the prototype and the optimal shape of the slots related to the approach 2

VI. Comparison of the results

In this paper, two considered approaches, which these approaches change the rotor slot dimensions, have been applied on a 30-kW squirrel cage induction motor (conventional model) to analyze the motor performance characteristics. These approaches with a combination of the genetic algorithm lead to an optimal model for the conventional model. The efficiency, power factor and starting torque are illustrated in Figure .13 to 15.

Based on Figure .13, the efficiency by both approaches 1, 2 are increased by 0.32% in comparison with the efficiency of the conventional model. Thus, based on efficiency, both approaches are the best.

The highest power factor is related to approach 2 which increased by 0.88% in comparison with the power factor of the conventional model (Figure .14).

Approach 2, has the highest starting torque than the other approach and the conventional model so that starting torque increased by 37.9% in comparison with the starting torque of the conventional model (Figure .15). Thus, according to the efficiency, power factor, and the starting torque, approach 2 is chosen as the best optimal approach. Also, the performance characteristics of the optimal model related to each approach are summarized in Table 8.

VII. Conclusions

The performance characteristics of the 3-phase, 30-kW, 4-pole squirrel cage induction motor (conventional model) have been calculated according to the mathematical equations. These equations are proportional to the magnetic equivalent circuit of the induction motor. The simulated results obtained from Maxwell software are close to the analytical and experimental results.

The sensitivity of the rotor slot dimensions showed that the rotor slot with the narrow top part, narrow bottom part, and the wide middle part has the highest efficiency. Also, the power factor for the slot with these characteristics is maximum. In addition, the starting torque is high when the top part of the slot is narrow.

Two different approaches have been applied to the conventional model to improve the motor performance characteristics such as efficiency, power factor and starting torque. These approaches include rotor slot dimensions (Approach 1), rotor slot shape (Approach 2). The genetic algorithm is employed to find the optimal model in each considered approach.

The efficiency, and starting torque by approach 1 are increased by 0.32%, and 18.13% whereas by approach 2 are increased by 0.32%, and 37.93%, respectively. Also, the power factor in approach 1 is reduced by 0.55% while it is almost constant in approach 2. Thus, based on the efficiency, power factor and starting torque, the optimal slot of prototype II in approach 2 has been chosen as the final optimal approach.

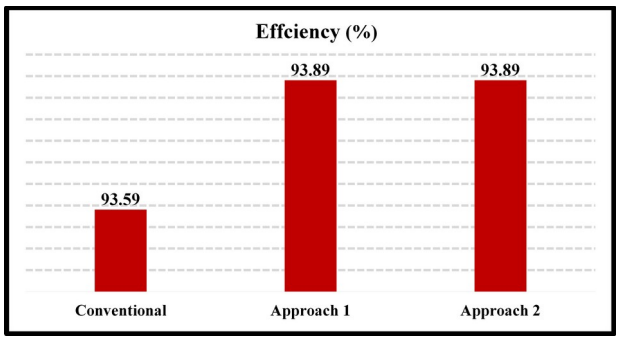

Figure 13. The efficiency of the considered approaches, and the conventional model

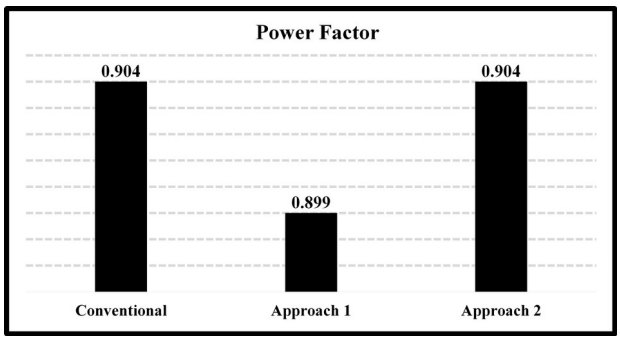

Figure 14. The power factor of the considered approaches, and the conventional model

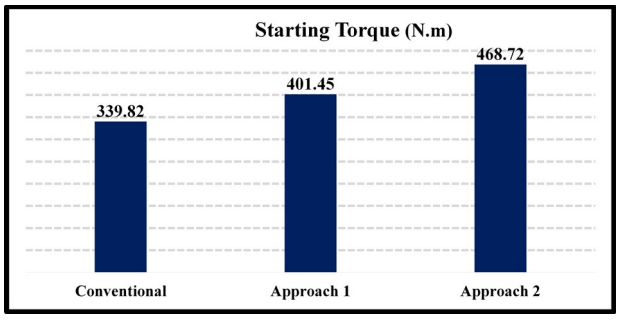

Figure 15. The starting torque of the considered approaches, and the conventional model

Table 8. The induction motor performance characteristics of optimal model related to the motor design approach in comparison with the conventional model (simulation results)

Characteristics	Conv.	Approach 1	Approach 2

η (%)	93.59	93.89	93.63
PF	0.904	0.899	0.912
I_{start} (A)	234.22	307.68	306.87
T_s (Nm)	339.82	401.45	468.72

VIII. Acknowledgment

This research was supported by the JEMCO company by providing information on a 30-kW induction motor.

IX. References

[1]. H.J.Lee, S.H.Im, D.Y.Um, and G.S.Park, "A Design of Rotor Bar for Improving Starting Torque by Analyzing Rotor Resistance and Reactance in Squirrel Cage Induction Motor," IEEE Trans. Magn., vol. 54, no. 3, March. 2018.

[2]. R.Parkash, M.J.Akhtar, R.K.Behra, S.K.Parida,'' Design of a Three Phase Squirrel Cage Induction Motor for Electric Propulsion Sys1tems'' Third International Conference on Advances in Control and Optimization of Dynamical Systems March 13-15, 2014. Kanpur, India.

[3]. H. Oraee 'A Quantitative Approach to Estimate the Life Expectancy of Motor Insulation Systems, IEEE Transaction on Dielectric and Electrical Insulation', vol. 7, No. 6, Dece. 2000.

[4]. H.M.Kim, K.W.Lee, D.G.Kim, J.H.Park, and G.S.Park," Design of Cryogenic Induction Motor Submerged in Liquefied Natural Gas " IEEE Trans. Mag., Vol. 54, No. 3, Mar. 2018.

[5]. D.Zhang, C.S.Park, and C.S.Koh, " A New Optimal Design Method of Rotor Slot of Three-Phase Squirrel Cage Induction Motor for NEMA Class D Speed-Torque Characteristic Using Multi-Objective Optimization Algorithm "IEEE Trans. Mag., Vol. 48, No. 2, Feb. 2012.

[6]. D.Lee and H.C.Jung, "Cost Pattern Value Method for Local Search Algorithms Applied to Optimal FEA-Based Design of Induction Motors" IEEE Trans. Magn, vol. 53, no. 11, Nov. 2018.

[7]. Z.Haisen, Z.Jian, W.Xiangyu, W.Qing, L.Xiaofang, and L.Yingli," A Design Method for Cage Induction Motors With Non-Skewed Rotor Bars " IEEE Trans. on Indus. Appl., Vol. 50, No. 2, Feb. 2014.

[8]. G.Lee, S.Min, and J.P.Hong, " Optimal Shape Design of Rotor Slot in Squirrel-Cage Induction Motor Considering Torque Characteristics " IEEE Trans. Mag., Vol. 49, No. 5, May. 2013.

[9]. J.Yun, and S.B.Lee, " Influence of Aluminum Die-Cast Rotor Porosity on the Efficiency of Induction Machines " IEEE Trans. Mag., Vol. 54, No. 11, Nov. 2018.

[10]. J.Yun, S.Lee, M.Jeong, and S.B.Lee, " Influence of Die Cast Rotor Fill Factor on the Starting Performance of Induction Machines " IEEE Trans. Mag., Vol. 54, No. 3, Mar. 2018.

[11]. D.J.Kim, J.W.Jung, J.P.Hong, K.J.Kim, and C.J.Park, " A Study on the Design Process of Noise Reduction in Induction Motors " IEEE Transaction on Indus. Appl., Vol. 48, No. 11, Nov. 2012.

[12]. L.Wang, X.Bao, C.Di and J.Li," Effects of Novel Skewed Rotor in Squirrel-Cage Induction Motor on Electromagnetic Force" IEEE Trans. Mag., vol. 51, no. 11, Nov. 2015.

[13]. C.G.Heo, H.M.Kim, and G.S.Park," A Design of Rotor Bar Inclination in Squirrel Cage Induction Machines" IEEE Trans. Mag., Vol. 51, No. 11, Nov. 2017.

[14]. Boldea and S. A. Nasar, 'The Induction Machines Design Handbook', 2nd ed. Boca Raton, Fl, USA: CRC Press, Dec 2010.